

Animations of progressive fibrous vein and fringe formation

D. KOEHN¹, P.D. BONNS², C. HILGERS³ & C.W. PASSCHIER²

¹Center for Advanced Studies, The Norwegian Academy of Science,
Drammensveien 78, N-0271 Oslo, Norway

²Tectonophysics, Institut für Geowissenschaften, Universität Mainz,
D-55099, Germany

³Geologie - Endogene Dynamik, RWTH Aachen,
D-52056, Germany

Abstract: We developed two programs, "Vein Growth" and "Fringe Growth", to investigate progressive growth of crystals in dilation sites (veins and strain fringes). Even though these models are based on a simple anisotropic growth function, they produce complex textures that compare well with natural examples of veins and strain fringes. In our simulations the most important factor that controls the crystal shape in the dilation site is the roughness of the growth surface (defined by asperities on the wall-rock of veins or core-object of fringe structures) and the amplitude of these asperities relative to the width of the dilation site after an opening-event. Fibrous crystals (crystals with a high length to width ratio) which can track the opening trajectory of the dilation site will develop if grain boundaries of crystals are locked to asperities on the wall-rock of veins or core-object of fringes. This happens only if the amplitude of the asperities is large relative to single opening steps of the dilation site and if crystals grow fast enough to close the site. The width of fibres depends on the number of initial nuclei and on the distance of adjacent asperities on the wall-rock- or core-object surface. Our simulations suggest that single fibres should not be used for structural analysis especially in the case of strain fringes since relative rotation between fringes and core-object influences fibre-growth directions. We discuss the implications of our modelling results for the use of crystal textures in veins and strain fringes for structural analysis.

keywords: vein, strain fringe, texture, fibre, crack-seal

Introduction

Veins and strain fringes are two types of dilation structures in which new crystals have grown (Durney and Ramsay, 1973; Ramsay and Huber, 1983; Passchier and Trouw, 1996; Bons, 2000). Veins are elongate dilation sites which normally form due to initial fracturing of the host-rock whereas strain fringes grow next to rigid objects at the site of the extensional instantaneous stretching axes of flow (ISA). A fringe structure consists of two fringes and a rigid core-object. Syndeformational crystal textures in veins and strain fringes are of great importance for structural analysis since they are thought to record part of the progressive deformation history of the host-rock (e.g. Durney and Ramsay, 1973; Ramsay and Huber, 1983; Ellis, 1986; Passchier and Trouw, 1996). Grain boundaries of crystals with high length to width ratios (fibres) are thought to follow the opening trajectory of veins and strain fringes. However, there are a number of uncertainties in fibre analysis since not all fibres grow in the direction of vein or fringe opening (Fig. 1, Cox and Etheridge, 1983; Fisher and Brantley, 1992; Bons and Jessell, 1997; Koehn and Passchier, 2000). Recently numerical experiments have been carried out to improve our understanding of crystal textures in dilation sites (Koehn et al., 2000, 2001; Bons, 2001; Hilgers et al., 2001) based on a crystal growth hypothesis put forward by Urai et al. (1991). In this paper we show some results of these studies in the form of movies in order to illustrate the progressive development of crystal textures in veins and strain fringes.

Veins or strain fringes can have either syntaxial, antitaxial, composite or ataxial growth of crystals (Durney and Ramsay, 1973; Hilgers et al., 2001). Syntaxial crystals grow in the dilation site from the wall-rock (veins) or from the core-object (strain fringes) and antitaxial crystals grow towards the wall-rock (veins) and towards the core-object (strain fringes). Composite growth is a mixture of antitaxial and syntaxial growth and ataxial growth describes growth at random sites within a fringe or vein.

We modelled mostly antitaxial growth where the growth surface is located between vein and host-rock or fringe and core-object. In addition to the location of their growth site, crystals in dilation sites are classified according to: 1) crystal shape and 2) crystal growth direction. Crystal shape



Figure 1. Crystal textures in a calcite, quartz and mica vein from the Orobic Alps (northern Italy). Crystals grew blocky to elongate and are not tracking the opening trajectory of the vein which is towards the lower left-hand side. Width of view is about 7mm.

is often used for veins whereas crystal growth direction is commonly used for strain fringes. Crystals can have a shape ranging from blocky to elongate or blade-like with a low length to width ratio (Fig. 1) to fibrous with a high length to width ratio (Fig. 2). Elongate crystals are commonly found in crack-seal veins with inclusion bands whereas fibrous crystals seldomly show inclusion bands. It is still not clear whether this means that fibrous crystals can develop in crack-seal veins or not. Crystals in strain fringes are generally considered fibrous (Fig. 3).

They are classified according to their growth direction ranging from displacement-controlled growth which means that fibres follow the opening path of the fringe to face-controlled where fibres grow normal to faces of the core-object. This classification has been extended by Koehn et al. (2000) by introducing "intermediate fibres" that switch between face- and displacement-controlled growth and "fibre bands" where face-controlled fibres grow within large displacement-controlled fibres.

In this paper we demonstrate how the numerical models "Vein Growth" and "Fringe Growth" (Koehn et al., 2000; Bons, 2001) can produce different crystal textures found in natural veins and strain fringes and discuss implications for structural analysis.

Programs

"Vein Growth" and "Fringe Growth" are based on a two-dimensional anisotropic growth function for crystal growth into dilation sites created by movement of rigid wall-rock (veins) and rigid core-objects (strain fringes; Koehn, 2000; Koehn et al., 2000; Bons 2001). The boundary of the "Vein Growth" model is the contact of crystals inside the vein towards the side which could either be represented by rigid wall-rock or neighbouring growing crystals (Fig. 4). The boundary of the "Fringe Growth" model is represented by the host-rock where new grains nucleate (Fig. 5). Parameters that can be changed during a run of the program are opening velocity and opening direction of the dilation site as well as growth velocity and anisotropy of growing crystals. Input parameters are a file describing the shape of the initial dilation site (shape of a fracture or crack for veins

and rigid core-object shape for fringes) and a file describing size and orientation of initial nuclei of growing crystals. Grains in the model are defined by nodes that are connected by straight line segments. Growth of grains is simulated by incremental movement of nodes into the open dilation site depending on the growth anisotropy of grains and their growth velocity. Nucleation of new grains takes place at the initial stage of vein or fringe opening, at the contact of fringes and veins to the wall-rock and inside fringes at the growth surface between two grains on a grain boundary. If wall-rock or parts of the object and growing crystals converge on each other, dissolution of vein/fringe crystals occurs. This is simulated by essentially the reverse of the growth routine. "Vein Growth" is described in detail in Bons (2001) and "Fringe Growth" in Koehn (2000) and Koehn et al. (2000). "Vein Growth" and "Fringe Growth" can be downloaded from the website, <http://www.uni-mainz.de/FB/Geo/Geologie/tecto/downloads/>.

"Vein Growth" mimicks the growth of one half of an antitaxial vein or of one crack-seal vein. The wall-rock can be moved away from the growing crystals in any desired xy direction on the computer screen. After an opening increment of the vein (wall-rock movement) crystals will grow into the open crack until they reach the wall-rock.

Figure 4 shows a movie of a simulation with a maximum crystal growth rate of 1 pixel/step and an opening of 2 pixels every 20 growth steps. The whole movie shows 1200 growth steps and 60 opening events with a picture taken after every 100th steps. Note that the growth rate of slowly growing crystals is not fast enough to seal the vein (right-hand side in figure 4). The developing crystal textures are described in more detail in section 3 of this paper.

"Fringe Growth" mimicks the growth of crystals in antitaxial strain fringes. Each of the two fringes of a fringe structure is simulated separately. The fringe is fixed in the computer reference frame (internal reference frame for a fringe structure; Koehn et al., 2000) and the core-object is moved in any desired xy direction on the screen and can be rotated around its center. Crystals keep on nucleating on the rims of the fringe. Figure 5 shows a simulation of "Fringe Growth" with 17500 growth steps and 500 fringe-opening events. The maximum crystal growth rate is 1.0 pixel/step



Figure 2. Fibrous calcite crystals with a high length to width ratio in a vein from a locality near Sestri Levante (Italy). Width of view is 10mm.

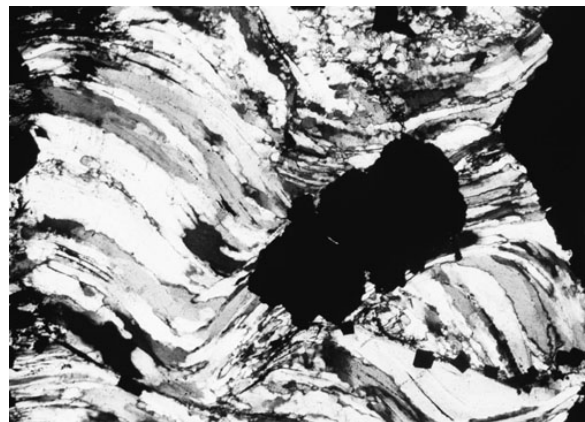


Figure 3. Fibrous quartz crystals between pieces of iron oxide from the Hamersley Ranges (Australia). Width of view is 8mm.

and the core-object moves 1.0 pixel away from the fringe every 30 growth steps. Crystal textures are described in more detail in section 3 of this paper. NOTE: length unit is "pixel" and time unit is "step"(representing one calculation step in the growth algorithm).

Textures

This section shows simulations of progressive crystal growth in veins and strain fringes and discusses the developing textures.

Veins

The first three simulations (Fig. 6 a-c) with "Vein Growth" show the development of crystal textures in one half of an antitaxial vein. The wall-rock surface is constructed using three sinusoidal-functions with different wavelengths (200, 60 and 12 pixels) and amplitudes (120, 40 and 8 pixels). Initial nuclei have a width of about 8 pixels. In all three simulations the vein first opens vertically until crystals have reached a steady state texture in terms of crystal width. Then vein opening changes by 20° towards



Figure 4. Simulation with the program "Vein Growth". The wall-rock is moved vertically towards the bottom of the figure in 60 opening events. Crystals grow to seal the open crack.

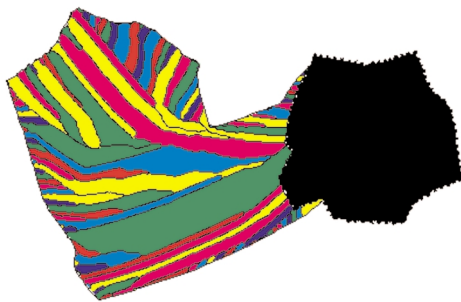


Figure 5. Simulation of antitaxial fibre growth in a strain fringe with the program "Fringe Growth". The fringe is fixed in the computer reference frame and the core-object is moved relative to the fringe and rotated around its center.

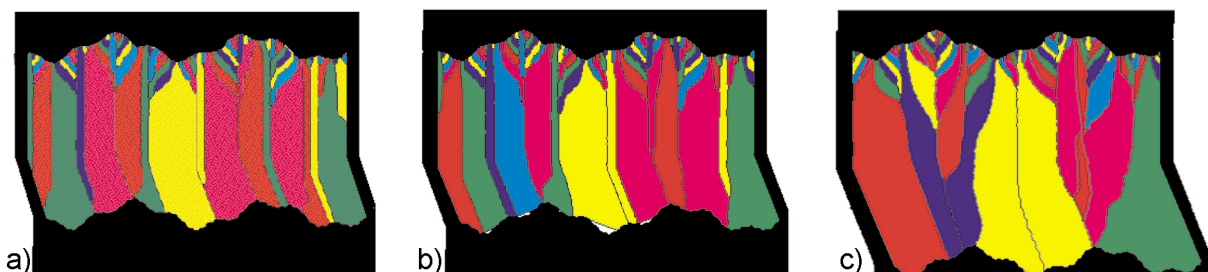


Figure 6. Three simulations with "Vein Growth" using different vein opening rates, a) Vein opening of 1 pixel every 20 growth stages; b) Vein opening of 2 pixels every 20 growth stages; c) Vein opening of 20 pixels every 200 growth stages.

the right reducing the tracking-capability of the host-rock asperities (Koehn et al., 2000). The maximum growth rate of crystals is 1.0 pixel/step in all simulations and vein opening velocity as well as opening amount per opening step was varied resulting in different textures.

The first simulation (Fig. 6a) shows 6000 growth stages with vein opening of one pixel every 20th growth stage resulting in 300 vein opening events. At the beginning of the simulation the number of growing crystals is reduced relatively fast with only some crystals surviving. After about 3000 growth stages crystals have reached a constant width and grain boundaries are locked to asperities on the host-rock surface. The width of different fibres is dependent on the distance between adjacent asperities which is a function of the different wave-lengths that describe the initial fracture surface. Therefore, the smallest fibres have a width of about 8 pixels and the largest a width of 40 pixels. After a change in the opening direction some fibre boundaries loose their connection to the wall-rock surface but most of them track vein opening.

The second simulation (Fig. 6b) lasts 3100 growth stages with the same number of growth steps per vein opening event as the first simulation (open every 20th growth stage) but with a larger vein-opening amount (2 pixels per opening step). With these settings, not all crystals grow fast enough to seal the vein completely. However, crystal textures are very similar to those of the first simulation (Fig. 6a) during vertical opening. Once the opening direction changes grain boundaries have less tracking capabilities as those in the first simulation.

The third simulation (Fig. 6c) lasts 4000 growth stages with an opening of the vein of 20 pixels every 200 growth events. The tracking capability of the asperities on the wall-rock surface is greatly reduced, even during vertical opening, since crystal growth is not as much restricted as it is in the first two simulations. This results in crystal textures similar to elongate blade-like crystals that can be found in typical crack-seal veins since crystals outgrow each other depending on their crystallographic orientation. However a few grain-boundaries are still tracking the vein opening and develop relatively large "fibrous" crystals. Their width is almost completely dependent on the largest wavelength that describes the wall-rock morphology of the vein because these asperities also have the largest amplitudes (120 pixels).

Figure 7a shows the simulation of a crack-seal vein with textures similar to striped bedding-veins found in the

Orobic Alps (Italy; Koehn and Passchier, 2000). The simulation shows 1000 growth steps with a maximum crystal growth rate of 1.0 pixel/step and a vein-opening of 10 pixels every 40 growth events. The resulting textures show elongate crystals that grow face-controlled and are not tracking the horizontal opening direction of the vein. The texture is very similar to the natural example shown in Figure 7b.

Strain Fringes

In this section we present six simulations that were performed with the program "Fringe Growth". Each figure is made up of two simulations, one for each fringe. We reoriented the simulations relative to an external reference frame (shear-zone boundary) assuming that fringes opened about parallel to the extensional ISA in simple shear flow with the flow plane oriented horizontally and a dextral sense of shear. In this case fringes and core-object rotate relative to the external reference frame as well as relative to each other. Note that we define relative rotation as rotation of the core-object around its centre relative to a fringe that is fixed in the internal reference frame (computer screen) so that core-object and fringes have different rotation rates relative to the external reference frame. Rotation rates for the simulations were taken from natural examples found in a locality near Lourdes (France) using the "object-centre path method" described in Koehn et al. (2001).

Figures 8 and 9 show simulations that illustrate the effect of internal nucleation and the effect of relative rotation between fringes and core-object on crystal textures. Figure 10 shows a simulation of fringes around a core-object from a natural fringe structure from a locality near Lourdes (France) described in detail in Koehn et al. (2001).

The simulation shown in figure 8 consists of 12000 growth stages with 400 opening events. Growth rate of crystals was 1.0 pixel/step and opening rate 1.0 pixel every 30 growth stages. Nucleation in the fringe was turned on so that crystals could nucleate on grain boundaries on the growth surface of the fringes. The simulation shows the development of face-controlled fibres, displacement-controlled fibres and intermediate fibres as well as the growth of fibre bands (Koehn et al., 2000, 2001). Running the movie in figure 8, it becomes evident which fibre parts are growing face- or displacement controlled and why some nuclei develop into fibre bands whereas others die out.

The simulation also illustrates the development of different crystal textures due to an asymmetric shape of the core-object, since both fringes in figure 8 rotated at the same rates relative to the external reference frame but show different internal textures and shapes.

Figure 9 illustrates the effect of rotation of core-objects (relative to their fringes) on the growth direction of displacement-controlled fibres. The simulation consists of 14000 growth steps with 349 fringe opening events, a growth rate of crystals of 1.0 pixel/step and an opening of 1.0 pixel every 40 growth steps. The core-object is rotating clockwise relative to the fringes and fringes and core-object

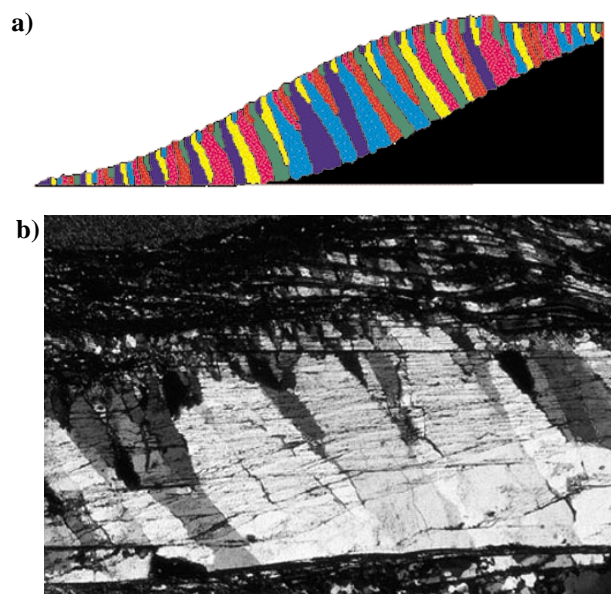


Figure 7. a) Simulation of crystal textures with the program "Vein Growth" to develop patterns found in striped bedding-veins from the Orobic Alps, Italy. b) Natural example of elongate crystals in a striped bedding-vein from the Orobic Alps. Sense of shear is sinistral, opening of the vein horizontal. Width of view is about 5mm.

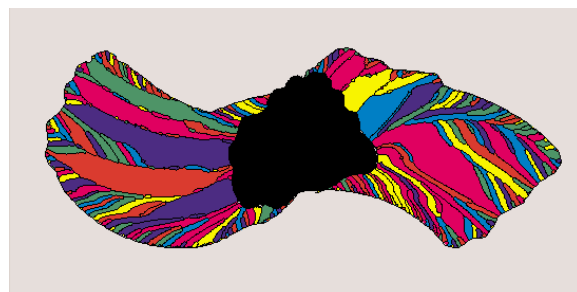


Figure 8. Simulation with the program "Fringe Growth" to illustrate growth of different fibre types in strain fringes. Fibre bands develop during nucleation of crystals on the growth surface of fringes.

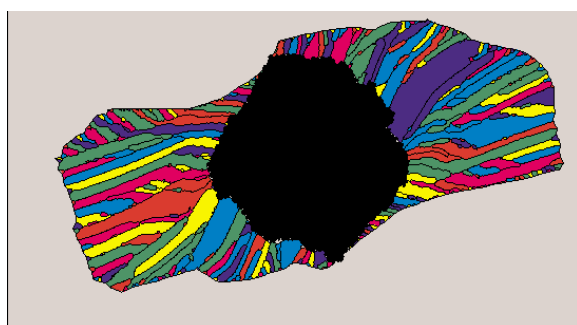


Figure 9. Simulation with the program "Fringe Growth" to illustrate the effect of relative rotation of core-object and fringes on growth direction of displacement-controlled fibres.

are changing their orientation relative to the external reference frame suddenly at growth step 10000.

After about 8000 growth steps the core-object has rotated 40° relative to its fringes. Displacement-controlled fibres next to the object (fibres of the same age) in the upper part of the right fringe have a different growth direction than

those in the lower part. This is an effect of relative rotation and shows that for these structures the growth direction of a single fibre cannot be used for a structural analysis (Koehn et al., 2000). Note that in this simulation both fringes are relatively similar in contrast to figure 8 since the core-object is almost equidimensional.

Figure 10a shows a natural fringes structure from Lourdes (France) and figure 10b a simulation of figure 10a with "Fringe Growth". The simulation consists of 6000 growth steps with 300 opening events, a growth rate of crystals of 1.0 pixel/step and an opening rate of the fringe of 1.0 pixel every 20 growth steps. The close similarity in textures between the model and the natural fringe structure supports the validity of the simulations. However if we use the assumption that fringes always open parallel to extensional ISA (Ellis, 1986) in figure 10 we have to induce sudden changes in rotation rate of fringes and core-object relative to ISA. This can have two possible causes: (1) polyphase deformation with sudden changes in ISA orientation with respect to the fringe structure (Aerden, 1996) or (2) fringes are not always opening parallel to extensional ISA (Koehn et al., 2001).

Structural Analysis

In this section we illustrate a method to interpret displacement-controlled fibre patterns in antitaxial strain fringes put forward by Aerden (1996) and Koehn et al. (2000; 2001). In this paper we argued that a single fibre should not be used for structural analysis since not all displacement-controlled fibres in a fringe grow in the same direction due to relative rotation of core-object and fringes. Therefore we use the "object-centre path method" to determine a fringe opening path that is independent of relative rotation and uses all fibres in a fringe. This method is illustrated in figure 11. To determine an object-centre path the core-object is moved relative to each fringe and rotated around its centre in a way that displacement-controlled fibres are always fixed to the same point on the core-object surface. The connection of the position of the core-object centre during this procedure defines the object-centre path. This path can now be used to calculate bulk shear strain of the matrix (Koehn et al., 2001). To illustrate fringe growth we can reorientate fringes and core-object with respect to the external reference frame (shear zone boundary) and develop a movie as shown in figure 12. In contrast to figures 6 - 10 of this paper where we assumed that fringes did always open parallel to extensional ISA of flow we now assume that they have a constant rotation rate between an initial position at the site of the extensional ISA and their final position. This produces a more realistic looking progressive development of the fringe structure where the opening direction varies relative to the extensional ISA. That this is a more realistic assumption has been shown by Koehn et al. (2000) with analog experiments of progressive fringe development. In their experiments, rotation rates did not change suddenly and the opening

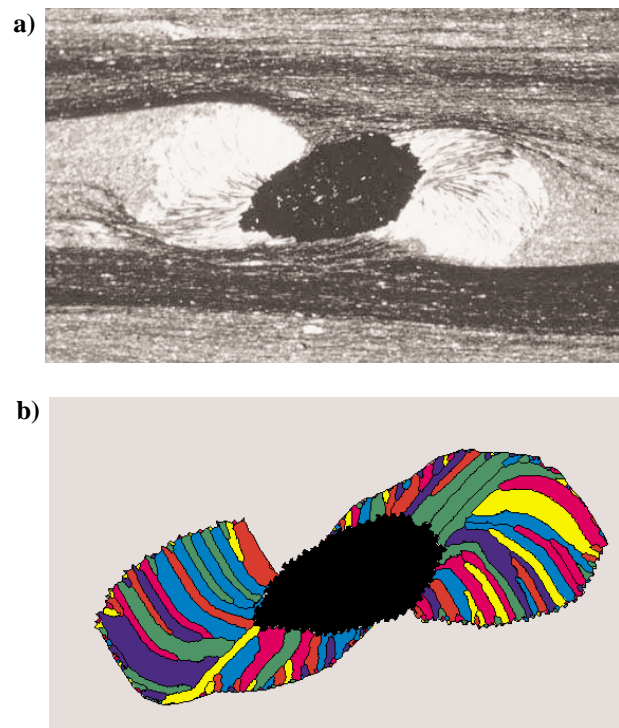


Figure 10. a) Natural example of a fringe structure from Lourdes. Width of view 20mm. b) Simulation of the fringe structure shown in (a) with the program "Fringe Growth".

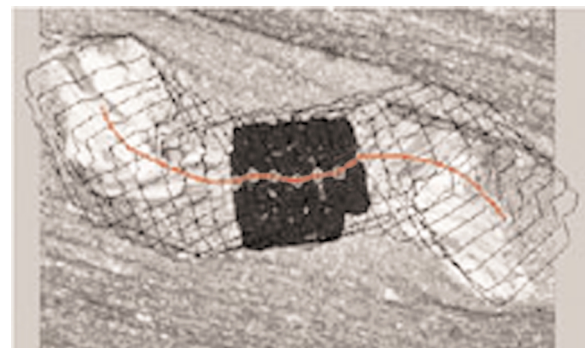


Figure 11. Movie illustrating how an object-centre path can be determined from a natural antitaxial strain fringe. The natural example is from a locality near Lourdes (France). Width of view is about 8mm.

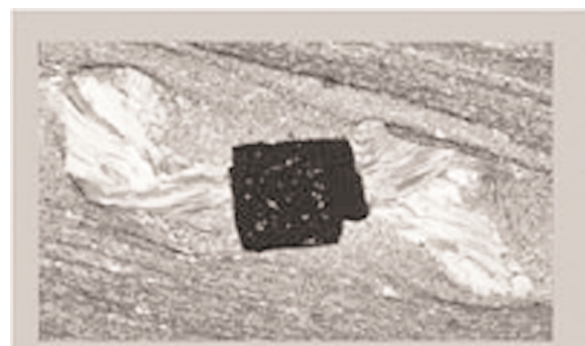


Figure 12. Movie illustrating the progressive development of the fringe structure shown in figure 11.

direction of fringes was not necessarily parallel to extensional ISA during progressive deformation.

Conclusions

Varied and often complex textures in veins and strain fringes can be realistically modelled (in 2 dimensions) with the programs "Vein Growth" and "Fringe Growth", respectively. The tracking capability of fibres depends mainly on the roughness of the growth surface, as crystal boundaries tend to lock onto asperities of the wall-rock or object surface (Urai et al., 1991). Displacement-controlled fibres thus track the relative movement between vein/fringe and wall-rock/object. This movement is not necessarily parallel to the extensional ISA and different displacement-controlled fibres may grow in different directions at the same time. Care should therefore be taken in the structural analysis of fibres, especially those in strain fringes. Single fibres should not be analysed in isolation. Instead, we propose the use of the "object-centre path method" that uses all fibres in a fringe.

Acknowledgements

This project benefited greatly from many discussions with Mark Jessell, Janos Urai and Domingo Aerden. The programs were initially developed at Monash University (Melbourne) with financial support from an Australian Research Council postdoctoral fellowship and subsequent Monash University Logan fellowship to Bons and DFG grant Pa 578/3 to Koehn and DFG grant ur-98-1-1 to Hilgers.

References

- AERDEN, D. G. A. M., 1996. The pyrite-type strain fringes from Lourdes (France): indicators of Alpine thrust kinematics in the Pyrenees. *Journal of Structural Geology* **18**, 75-91.
- BONS, P. D., JESSELL, M.W., 1997. Experimental simulation of the formation of fibrous veins by localised dissolution-precipitation creep. *Mineralogical Magazine* **61**, 53-63.
- BONS, P. D., 2000. The formation of veins and their microstructures. In: Stress, Strain and Structure, A volume in honour of W.D.Means. Eds: M.W.Jessell and J.L.Urai. *Journal of the Virtual Explorer* **2**.
- BONS, P. D., 2001. Development of crystal morphology during unitaxial growth in a progressively widening vein: I. The numerical model. *Journal of Structural Geology*, **23**, 865-872.
- COX, S. F. & ETHERIDGE, M. A., 1983. Crack-seal fibre growth mechanisms and their significance in the development of oriented layer silicate microstructures. *Tectonophysics*, **92**, 147-170.
- DURNEY, D. W. & RAMSAY, J.G., 1973. Incremental strains measured by syntectonic crystal growths. In: DeJong, K.A., Scholten, R. (Eds), *Gravity and Tectonics*, Wiley, NY, 67-95.
- ELLIS, M. A., 1986. The determination of progressive deformation histories from antitaxial syntectonic crystal fibres. *Journal of Structural Geology* **8**, 701-709.
- FISHER, D. M., BRANTLEY, S.L., 1992. Models of quartz overgrowth and vein formation: deformation and episodic fluid flow in an ancient subduction zone. *Journal of Geophysical Research* **97**, 20043-20061.
- HILGERS, C., KOEHN, D., BONNS, P. D. & URAI, J. L., 2001. Development of crystal morphology during unitaxial growth in a progressively widening vein: II. Numerical simulations of the evolution of antitaxial fibrous veins. *Journal of Structural Geology*, **23**, 873-885.
- KOEHN, D., BONNS, P. D., PASSCHIER, C. W., 2000. Numerical and experimental modelling of strain fringes, *Geoscience* 200, Manchester, Abstract Volume **126**.
- KOEHN, D., PASSCHIER, C. W., 2000. Shear sense indicators in striped bedding-veins. *Journal of Structural Geology* **22**, 1141-1151.
- KOEHN, D. 2000. Kinematics of fibrous aggregates. Phd-thesis, Mainz University.
- KOEHN, D., HILGERS, C., BONNS, P. D. & PASSCHIER, C. W., 2000. Numerical simulation of fibre growth in antitaxial strain fringes. *Journal of Structural Geology*, **22**, 1311-1324.
- KOEHN, D, AERDEN, D. G. A. M., BONNS, P. D. & PASSCHIER, C. W., 2001. Computer experiments to investigate complex fibre patterns in natural antitaxial strain fringes. *Journal of Metamorphic Geology*, **19**, 217-231.
- PASSCHIER, C. W., TROUW, R. A. J., 1996. *Microtectonics*. Springer, Heidelberg.
- RAMSAY, J. G. & HUBER, M. I., 1983. The techniques of modern structural geology, 1: Strain analysis. *Academic Press*, London.
- URAI, J. L., WILLIAMS, P. F. & VAN ROERMUND, H. L. M., 1991. Kinematics of crystal growth in syntectonic fibrous veins. *Journal of Structural Geology* **13**, 823-836.